^{59}Co NMR evidence for charge ordering below $T_{CO} \sim 51$ K in $\mathbf{Na_{0.5}CoO_2}$

F. L. Ning[1], S. M. Golin[1], K. Ahilan[1], T. Imai[1,2], G.J. Shu[3], and F. C. Chou[3,4]

[1]*Department of Physics and Astronomy, McMaster University, Hamilton, Ontario L8S 4M1, Canada*
[2]*Canadian Institute for Advanced Research, Toronto, Ontario M5G1Z8, Canada*
[3]*Center for Condensed Matter Sciences, National Taiwan University, Taipei 10617, Taiwan and*
[4]*National Synchrotron Radiation Research Center, HsinChu 30076,Taiwan*
(Dated: February 2, 2008)

The CoO$_2$ layers in sodium-cobaltates Na$_x$CoO$_2$ may be viewed as a spin $S = \frac{1}{2}$ triangular-lattice doped with charge carriers. The underlying physics of the cobaltates is very similar to that of the high T_c cuprates. We will present unequivocal ^{59}Co NMR evidence that below $T_{CO} \sim 51$ K, the insulating ground state of the itinerant antiferromagnet Na$_{0.5}$CoO$_2$ ($T_N \sim 86$ K) is induced by charge ordering.

PACS numbers: 71.27.+a, 71.30.+h, 76.60.-k

The discovery of unconventional superconductivity in sodium-cobaltate Na$_{1/3}$CoO$_2$[H$_2$O]$_{4/3}$ ($T_c \sim 4.5$ K) [1, 2, 3] has generated major excitement in the condensed matter community. Co ions in the CoO$_2$ layers take a mixed valence state Co^{+4-x}, and form a triangular-lattice. Since Co^{4+} and Co^{3+} ions nominally have spins of $S = \frac{1}{2}$ and $S = 0$, respectively, one may consider the CoO$_2$ layers as a $S = \frac{1}{2}$ triangular-lattice doped with charge carriers, in analogy with the doped CuO$_2$ square-lattice in the high T_c cuprate superconductors. The fingerprints of Co spins are everywhere in Na$_x$CoO$_2$: Na$_{0.82}$CoO$_2$ is an itinerant antiferromagnet ($T_N \sim 21$ K) [4]; Na$_{0.7}$CoO$_2$ is a "Curie Weiss metal" with large paramagnetic susceptibility [5]; Na$_{0.5}$CoO$_2$ is an itinerant antiferromagnet ($T_N \sim 86$ K) [5], and undergoes a mysterious metal-insulator transition below ~ 51 K [5].

In the case of the cuprates, doped holes tend to segregate themselves from the underlying $S = \frac{1}{2}$ square-lattice to form static *charge stripes* [6]. Whether the charge ordering in stripes is related to or competing against the mechanism of high T_c superconductivity is controversial [7]. A major question we address here is whether or not the cobaltates also exhibit a similar phenomenon in the triangular-lattice geometry. The insulating ground state of Na$_{0.5}$CoO$_2$ below ~ 51 K has attracted considerable attention because of speculation that it may be charge ordered [5, 8, 9, 10]. However, earlier ^{23}Na NMR measurements in Na$_{0.5}$CoO$_2$ showed no evidence of the emergence of a charge ordered state below ~ 51 K [11, 12, 13].

In this *Letter*, we take a more direct approach to probing the charge environment in CoO$_2$ layers, by measuring the EFG (*Electric Field Gradient*) of Co sites with zero-field ^{59}Co NMR. The EFG tensor is the second derivative of the Coulomb potential, and hence is directly related to the local charge density. We will present unequivocal evidence that the insulating ground state of Na$_{0.5}$CoO$_2$ below $T_{CO} \sim 51$ K is indeed the consequence of charge ordering.

A major distinction between cobaltates and cuprates is that the Na$^+$ ions in cobaltates can spatially order for certain values of Na concentration, x. Besides donating electrons, ordered Na$^+$ ions exert a pe-

riodic Coulomb potential on the CoO$_2$ triangular-lattice [5, 14, 15, 16, 17, 18]. In the case of Na$_{0.5}$CoO$_2$, electron and neutron diffraction measurements have suggested that Na$^+$ ions form zigzag chains [5, 14, 15]. This results in the presence of two structurally inequivalent Co sites, each forming a chain structure[15] as shown in Fig. 1. One of the nearest neighbor sites of Co(1) is occupied by a Na$^+$ ion, while Co(2) has no Na$^+$ ions in the nearest neighbor sites [15]. Since the Coulomb potential from Na$^+$ chains attracts electrons, the valence of Co(1) sites, Co$^{+3.5-\delta}$, is smaller than that of Co(2) sites, Co$^{+3.5+\delta}$. The average valence of Co ions in Na$_{0.5}$CoO$_2$ is $+3.5$. The valence of Co(2) sites is closer to Co^{+4} ($S = \frac{1}{2}$), hence Co(2) exhibits strong spin fluctuations above $T_N \cong 86$ K [19], and develops a sizable ordered magnetic moment $\sim 0.26\mu_B$ within the CoO$_2$ plane below T_N [9, 20]. On the other hand, Co(1) sites have much weaker spin fluctuations above T_N[19]. The upper bound of the ordered moment at Co(1) sites is as small as $\sim 0.04\mu_B$ at 8 K and too small to be detected by polarized neutron scattering techniques [9]. ^{59}Co zero field NMR is a very powerful technique for detecting small hyperfine magnetic field B_{hf}, which is proportional to the ordered magnetic moments. Yokoi et al. took advantage of this high sensitivity, and demonstrated the presence of small ordered moments at Co(1) sites along the crystal c-axis below $T_N \sim 86$ K. This led them to propose two possible spin structures as shown in Fig.1 [20].

Although the existence of multiple Co sites in Na$_x$CoO$_2$ is sometimes referred to as a consequence of *charge ordering* persisting up to room temperature, it is important to realize that these distinct behaviors of Co(1) and Co(2) sites in Na$_{0.5}$CoO$_2$ are directly linked with the periodic Coulomb potential arising from Na$^+$ zigzag chains. Moreover, charges on the Co sites are mobile, and Na$_{0.5}$CoO$_2$ is metallic above $T_{CO} \sim 51$ K [5]. In contrast, strong electron-electron correlation effects in high T_c cuprates induce a self-organized pattern of doped carriers in the form of charge stripes [6]. The spatial periodicity of the charge ordered state is different from that of the Coulomb potential of the underlying lattice. It is this type of self-organized charge pattern that we are

searching for in $Na_{0.5}CoO_2$.

In Fig.2, we present typical zero-field ^{59}Co (nuclear spin $I = \frac{7}{2}$) NMR lineshapes from a piece of electro-chemically deintercalated $Na_{0.5}CoO_2$ single crystal (mass $\sim$ 25mg) [21, 22]. The observed lineshapes are similar to Yokoi's[20]. Below $T_N \sim 86\ K$, we observe 7 NMR peaks of Co(2) sites for transitions between nuclear spin $I_z = \frac{2m+1}{2}$ and $I_z = \frac{2m-1}{2}$, where integer $-3 \le m \le +3$. In the frequency range above 5 MHz, we have also successfully detected Co(1) zero-field NMR signals for the $m = 0$ to $m = +3$ transitions. The intensity of NMR signals decreases in proportion to the square of the frequency, and measurements below 5 MHz are formidable. We summarize the temperature dependence of the observed peak frequencies f_m of Co(1) sites in Fig.3. A remarkable feature of Fig.2 and Fig.3 is that all 4 peaks of Co(1) sites split into two precisely below $T_{CO} \sim 51$ K. In contrast, Co(2) sites show no anomalies. In what follows, we will refer to the two inequivalent Co(1) sites as Co(1a) and Co(1b). In passing, the comparison between the zero-field and low-field NMR lineshapes indicates that the NMR signals near 6 MHz, shown in green, are not related to Co(1) sites [13]. We tentatively attribute these unidentified signals to defect sites caused by slight deviation of Na concentration from 0.5 and/or minor disorder. We also confirmed that both Co(1a) and Co(1b) lines split in weak magnetic field applied along the c-axis [13]. This means that both Co(1a) and Co(1b) sites have up-spins as well as down-spins.

To understand the effects of the EFG on NMR lineshapes, we need to theoretically compute the resonance frequency f_m of the m-th transition as $f_m = (E_{(2m+1)/2} - E_{(2m-1)/2})/h$, where the energy levels E_n are eigenvalues of the standard ^{59}Co nuclear spin Hamiltonian,

$$H = \frac{h\nu_Q^Z}{6}\{3I_Z^2 - I(I+1) + \eta(I_X^2 - I_Y^2)\} - \gamma_n h\mathbf{B}\cdot\mathbf{I}.\ \ (1)$$

The first term of the Hamiltonian represents the nuclear quadrupole interaction [23] between the EFG and the ^{59}Co nuclear quadrupole moment. The diagonalized tensor of the nuclear quadrupole interaction (ν_Q^X, ν_Q^Y, ν_Q^Z) is proportional to the EFG tensor ($d\phi^2/dX^2$, $d\phi^2/dY^2$, $d\phi^2/dZ^2$), where ϕ is the total Coulomb potential seen by ^{59}Co nuclei, and X, Y and Z represent three orthogonal, principal axes (by following the convention, we define $|\nu_Q^X| < |\nu_Q^Y| < |\nu_Q^Z|$). From the comparison of zero-field NQR (Nuclear Quadrupole Resonance) results at 110 K (see Fig.2) and high-field NMR, we found that the main-principal axis Z coincides with the crystal c-axis within experimental uncertainties ($\sim$ 5 degrees). This means that the other principal axes, X and Y, lie within the CoO_2 plane. Poisson's relation for the Coulomb interaction sets a constraint, $\nu_Q^X + \nu_Q^Y + \nu_Q^Z = 0$. Hence we have only two independent parameters in the first term of eq.(1), ν_Q^c (we now denote $Z = c$) and the anisotropy parameter $\eta = (\nu_Q^Y - \nu_Q^X)/\nu_Q^Z$. η is a measure of the deviation from axial symmetry of the EFG tensor with respect

to the crystal c-axis. In the paramagnetic state at 110 K ($> T_N$), we deduced from the ^{59}Co NQR lineshape that $\nu_Q^c = 2.799(5)$ MHz and $\eta = 0.300(1)$ for Co(1) sites, and $\nu_Q^c = 4.040(5)$ MHz and $\eta = 0.400(1)$ for Co(2) sites.

The second term in the Hamiltonian represents the Zeeman interaction between Co nuclear spins and the *local* magnetic field, $\mathbf{B}$, at the position of the observed nuclear spin. $\gamma_n = 2\pi \times 10.054$ MHz/Tesla is the ^{59}Co nuclear gyromagnetic ratio. In our zero-field NMR measurements, we apply no external magnetic field. Hence $\mathbf{B} = \mathbf{B}_{hf}$, where $\mathbf{B}_{hf}$ is the hyperfine magnetic field from ordered Co moments. $\mathbf{B}_{hf}$ is proportional to the sublattice magnetization, $\mathbf{M}(T)$, of Co sites [20]. The $m = 0$ transition frequency depends primarily on the Zeeman term, $f_0 \sim \gamma_n|\mathbf{B}_{hf}|$. At 60 K, $f_0 = 6.659$ MHz and 19.780 MHz for Co(1) and Co(2) sites, respectively, because the hyperfine magnetic field is $|\mathbf{B}_{hf}| \sim 0.6$ Tesla at Co(1) sites, and ~ 1.9 Tesla at Co(2) sites. The separation between adjacent peaks, $(f_{m+1} - f_m)$, depends primarily on the EFG. For Co(1) sites, $(f_{m+1} - f_m) \sim \nu_Q^c \sim 2.8$ MHz, since the ordered moments point along the c-axis. For Co(2) sites, the separation is $(f_{m+1} - f_m) \sim \nu_Q^{a,b} \sim \nu_Q^c/2 \sim 2$ MHz or less, because the ordered magnetic moments point within the ab-plane. The observed peaks f_m are not evenly spaced, because the nuclear quadrupole and Zeeman interactions are comparable in the present case. This means that we must diagonalize the Hamiltonian in eq.(1) exactly to fit the lineshapes. By relying on inaccurate second-order perturbation analysis, Yokoi et al. not only misidentified the peaks of Co(2) sites but were also unable to deduce the critically important information associated with the Co(1) sites [20].

Based on the exact diagonalization, we matched all the observed zero-field NMR peaks with theoretically calculated values of f_m as shown by vertical lines in Fig.2. This allowed us to deduce the relevant NMR parameters of eq.(1), *i.e.* ν_Q^c, η, the magnitude of B_{hf}, and the relative polar angle (θ, ϕ) between B_{hf} and the c-axis. We found that η shows no temperature dependence across 51 K, and (θ, ϕ) change less than 2 degrees from the values at 60 K ($\theta = 9 \pm 1°$, $\phi = 0°$). Hence we focus our attention on the temperature dependence of ν_Q^c and B_{hf} of Co(1a) and Co(1b) sites.

Co(1a) and Co(1b) have different values of ν_Q^c, as shown in Fig4b. This is direct proof that local charge environment is different between Co(1a) and Co(1b) sites. In principle, a differentiation of the EFG between Co(1a) and Co(1b) sites could arise if a structural phase transition doubles the unit cell of Na^+ zigzag chains. To rule out such a scenario, we deduced $\nu_Q^c(Na)$ at two structurally inequivalent Na sites, Na(1) and Na(2) [15], from the measurements of $+\frac{1}{2}$ to $-\frac{1}{2}$ central transition and $\pm\frac{3}{2}$ to $\pm\frac{1}{2}$ satellite transitions of ^{23}Na NMR in the same crystal [13]. As summarized in Fig.4a, we found no hint of additional splitting or extra broadening for $\nu_Q^c(Na)$ below T_{CO}. The upper bound of the potential splitting of $\nu_Q^c(Na)$ at 4 K is less than $\sim 1\%$, while

the splitting of ν_Q^c between Co(1a) and Co(1b) sites, $\Delta\nu_Q^c = \nu_Q^{c,\,Co(1b)} - \nu_Q^{c,\,Co(1a)}$, reaches as much as $\sim 6\%$, as shown in Fig.4d. Therefore we conclude that *Co(1) sites undergo a charge ordering transition at* $T_{CO} \sim 51$ *K.*

The observed differentiation of B_{hf} between Co(1a) and Co(1b) sites in Fig.4c is also understandable as a consequence of charge ordering. Since the valence state is different below $T_{CO} \sim 51$ K, the number of electrons filling the t_{2g} orbitals of Co(1a) and Co(1b) sites will also be different. This naturally results in a different magnitude of ordered moments at Co(1a) and Co(1b) sites, and hence separate values of B_{hf}. In Fig.4d, we plot the splitting of B_{hf} between Co(1a) and Co(1b) sites, $\Delta B_{hf} = B_{hf}^{Co(1a)} - B_{hf}^{Co(1b)}$. ΔB_{hf} shows an identical temperature dependence as $\Delta\nu_Q^c$ within experimental uncertainties. This is not surprising, because to a good approximation, both $\Delta\nu_Q^c$ and ΔB_{hf} should be proportional to the difference of the number of electrons occupying the Co 3d orbitals. Thus we may consider $\Delta\nu_Q^c$ and ΔB_{hf} as *the order parameter* of charge ordering below 51 K. By fitting the temperature dependence down to 40 K ($= 0.8T_{CO}$) to a typical power law behavior, $\Delta\nu_Q^c \sim \Delta B_{hf} \sim (T - T_{CO})^{\beta'}$, we found the critical exponent $\beta' = 0.3 \pm 0.1$. Interestingly, this value is comparable to the critical exponent $\beta = 0.28 \pm 0.02$ observed for the sub-lattice magnetization, $M(T) \sim (T - T_N)^{\beta}$ at $T_N = 86$ K for the antiferromagnetic Néel transition of Co(2) sites [9].

To conclude, we have presented unequivocal zero-field NMR evidence that static differentiation of charge densities develops below $T_{CO} \sim 51$ K in the one dimensional chain structure of Co(1) sites. In contrast, Co(2) sites have only spin ordering and show no anomalies either in NMR lineshapes or ν_Q across 51 K. In Fig.1, we show the possible charge ordering patterns with the smallest possible unit cell. Our observation of a striped configuration of the charge ordered state, consisting of Co(1) chains with charge and spin ordering and Co(2) chains with spin ordering only, is consistent with the two-fold symmetry observed for in-plane magnetoresistance by Balicas et al. [8]. The splitting of ν_Q^c (and hence EFG) reaches as much as ~ 6 % between Co(1a) and Co(1b) sites. We recall that ν_Q^c at ^{63}Cu sites increases by $\sim 10\%$ in high T_c cuprates when the hole concentration x changes by 0.15 in the CuO$_2$ plane of La$_{2-x}$Sr$_x$CuO$_4$ [24]. If we assume that the charge doping effects on the EFG are comparable between cobaltates and cuprates, we can crudely estimate the differentiation of the valence between Co(1a) and Co(1b) sites as ~ 0.1. It is worth noting that t-U-V model calculations [10] showed that *a differentiation of valence of Co(2) sites as little as* ~ 0.03 *may be sufficient to drive* CoO$_2$ *planes into insulating.* On the other hand, none of the charge ordered patterns proposed within the existing theoretical frameworks [10, 25, 26] are consistent with our experimental finding of charge ordering *on Co(1) sites.* Clearly, more theoretical works are required.

[1] K. Takada, H. Sakurai, E. Takayama-Muromachi, F. Izumi, R. Dilanian, and T. Sasaki, Nature **422**, 53 (2003).

[2] T. Fujimoto, G. Q. Zheng, Y. Kitaoka, R. L. Meng, J. Cmaidalka, and C. W. Chu, Phys. Rev. Lett. **92**, 047004 (2004).

[3] K. Ishida, Y. Ihara, Y. Maeno, C. Michioka, M. Kato, K. Yoshimura, K. Takada, T. Sasaki, H. Sakurai, and E. Takayama-Muromachi, J. Phys. Soc. Jpn. **72**, 3041 (2003).

[4] S. P. Bayrakci, I. Mirebeau, P. Bourges, Y. Sidis, M. Enderle, J. Mesot, D. P. Chen, C. T. Lin, and B. Keimer, Phys. Rev. Lett. **94**, 157205 (2005).

[5] M. L. Foo, Y. Y. Wang, S. Watauchi, H. W. Zandbergen, T. He, R. J. Cava, and N. P. Ong, Phys. Rev. Lett. **92**, 247001 (2004).

[6] J. M. Tranquada, B. J. Sternlieb, J. D. Axe, Y. Nakamura, and S. Uchida, Nature **375**, 561 (1995).

[7] A. J. Millis and J. Orenstein, Science **288**, 468 (2000).

[8] L. Balicas, M. Abdel-Jawad, N. E. Hussey, F. C. Chou, and P. A. Lee, Phys. Rev. Lett. **94**, 236402 (2005).

[9] G. Gasparovic, R. A. Ott, J. H. Cho, F. C. Chou, Y. Chu, J. W. Lynn, and Y. S. Lee, Phys. Rev. Lett. **96**, 046403 (2006).

[10] S. Zhou and Z. Wang, Phys. Rev. Lett. **98**, 226402 (2007).

[11] B. Pedrini, J. L. Gavilano, S. Weyeneth, J. Hinderer, M. Weller, H. R. Ott, S. M. Kazakov, and J. Karpinski, Phys. Rev. B **72**, 214407 (2005).

[12] J. Bobroff, G. Lang, H. Alloul, N. Blanchard, and G. Collin, Phys. Rev. Lett. **96**, 107201 (2006).

[13] F. L. Ning, unpublished.

[14] H. W. Zandbergen, M. Foo, Q. Xu, V. Kumar, and R. J. Cava, Phys. Rev. B **70**, 024101 (2004).

[15] Q. Huang, M. L. Foo, R. A. Pascal, J. W. Lynn, B. H. Toby, T. He, H. W. Zandbergen, and R. J. Cava, J. Phys. Condens. Matter **16**, 5803 (2004).

[16] P. H. Zhang, R. B. C. ad M. L.Čohen, and S. G. Louie, Phys. Rev. B **71**, 153102 (2005).

[17] M. Roger, D. J. P. Morris, D. A. Tennant, M. J. Gutmann, J. P. Goff, J. U. Hoffman, R. Feyerherm, E. Dudzik, D. Prahakaran, A. T. Boothroyd, et al., Nature **445**, 631 (2007).

[18] F. C. Chou, M.-W. Chu, G. Shu, F. T. Huang, W. W. Pai, H. S. Sheu, T. Imai, F. L. Ning, and P. A. Lee, arXiv:0709.0085.
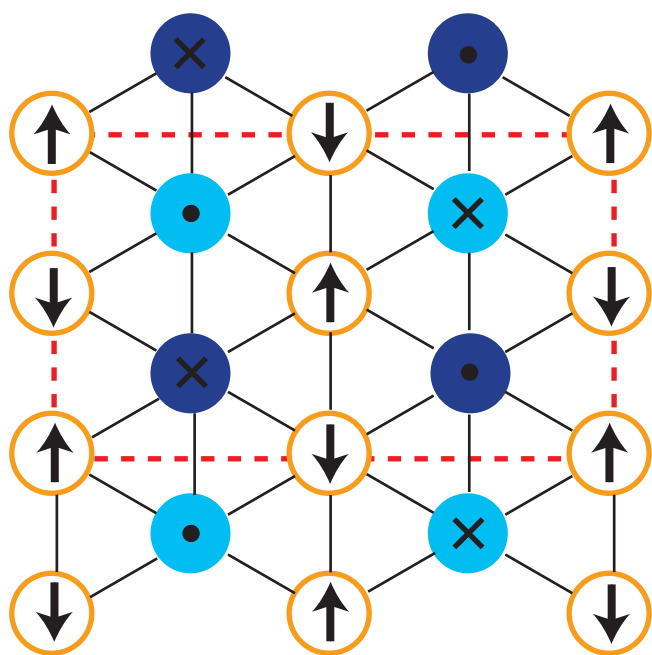
[19] F. L. Ning, T. Imai, B. W. Statt, and F. C. Chou, Phys.

Rev. Lett. **93**, 237201 (2004).

[20] M. Yokoi, T. Moyoshi, Y. Kobayashi, M. Soda, Y. Yasui, M. Sato, and K. Kakurai, J. Phys. Soc. Jpn. **74**, 3046 (2005).

[21] G. J. Shu, A. Prodi, S. Y. Chu, Y. S. Lee, H. S. Sheu, and F. C. Chou, arXiv:0708.0280.

[22] F. C. Chou, J. H. Cho, P. A. Lee, E. T. Abel, K. Matan, and Y. S. Lee, Phys. Rev. Lett. **92**, 157004 (2004).

[23] T. P. Das and E. L. Hahn, Solid State Physics, Supplement **1**, 1 (1958).

[24] T. Imai, C. P. Slichter, K. Yoshimura, and K. Kosuge, Phys. Rev. Lett. **70**, 1002 (1993).

[25] H. Watanabe and M. Ogata, J. Phys. Soc. Jpn. **75**, 063702 (2006).

[26] T. P. Choy, D. Galanakis, and P. Philips, Phys. Rev. B **75**, 073103 (2007).

Fig.1. Ordered magnetic moments on Co(1) sites point either *up* ($\bullet$) or *down* ($\times$), while moments on Co(2) sites point within the plane (arrows) [20]. Co(1) sites have either in-plane antiferromagnetic order (left panel) or in-plane ferromagnetic order (right panel). In the latter case, Co(1) sites in the adjacent CoO_2 layers have opposite spin orientation. Dark blue and light blue on Co(1a) and Co(1b) sites, respectively, represent possible charge ordering patterns to be determined in this work. Red dashed lines represent the unit cell in each possible configuration.

Fig.2. ^{59}Co NMR lines at Co(1) sites (blue) and Co(2) sites (orange) at 110 K (paramagnetic state, $B_{hf} = 0$), 60 K (Néel ordered state), 30 K and 4.2 K (charge ordered state). Vertical lines represent theoretical fit of resonance frequencies f_m for Co(1) (black), Co(1a) (dark blue), Co(1b) (light blue), and Co(2) (orange). Peak(s) near 6 MHz (green) are not associated with Co(1) or Co(2) sites (see main text).

Fig.3. f_m ($m = 0, 1, 2$ and 3) for Co(1) (black) above T_{CO}, and Co(1a) (dark blue) and Co(1b) (light blue) below T_{CO}. Vertical arrows roughly represent the magnitude of ν_Q^c for Co(1a) and Co(1b) sites.

Fig.4. (a) Temperature dependence of $\nu_Q^c(Na)$ at Na(1) and Na(2) sites. The distribution of $\nu_Q^c(Na)$ is about the size of the symbols. (b) Temperature dependence of ν_Q^c, and (c) hyperfine field B_{hf} in Co(1) sites. Color convention is the same as in Fig.2 and Fig.3. (d) $\Delta\nu_Q^c$: the splitting of ν_Q^c between Co(1b) and Co(1a) sites deduced from Fig.4b (left axis, diamond). ΔB_{hf} : the splitting of B_{hf} between Co(1a) and Co(1b) deduced from Fig.4c (right axis, filled circles). Solid curve shows a best fit to $\Delta\nu_Q^c \sim \Delta B_{hf} \sim (T - T_{CO})^{\beta'}$ with a critical exponent $\beta' = 0.3$. The dashed line shows $T_{CO} \sim 51\ K$.

Co(1a) Co(1b) Co(2)

m=
±2 ±1 ±2 ±3   ±3

110 K
(NQR)

60 K

30 K

4.2 K

m= 0   1   2   3 -3   -2   -1   0 1 23

Frequency [MHz]